Journal of Photochemistry & Photobiology, B: Biology 224 (2021) 112306

Contents lists available at ScienceDirect

Journal of Photochemistry & Photobiology, B: Biology

journal homepage: www.elsevier.com/locate/jphotobiol

Effects of water-filtered infrared A and visible light (wIRA/VIS) radiation on heat- and stress-responsive proteins in the retina and cornea of guinea pigs

Antonia Frohns [a], Marijana Stojanovic [b], Talin Barisani-Asenbauer [c], Jasmin Kuratli [d], Nicole Borel [d], Aleksandra Inic-Kanada [c,*]

[a] Technical University of Darmstadt, Darmstadt, Germany
[b] Institute of Virology, Vaccines and Sera - TORLAK, Belgrade, Serbia
[c] Institute of Specific Prophylaxis and Tropical Medicine, Center for Pathophysiology, Infectiology and Immunology, Medical University of Vienna, Vienna, Austria
[d] Institute of Veterinary Pathology, (IVPZ) and Center for Applied Biotechnology and Molecular Medicine (CABMM), Vetsuisse Faculty, University of Zurich, Zurich, Switzerland

ARTICLE INFO

Keywords:
wIRA/VIS
In vivo
guinea pig
Retina
Cornea

ABSTRACT

Water-filtered infrared A and visible light (wIRA/VIS), shown to reduce chlamydial infections *in vitro* and *in vivo*, might represent an innovative therapeutic approach against trachoma, a neglected tropical disease caused by ocular infection with the bacterium *C. trachomatis*. In this *in vivo* study, we assessed the impact of wIRA radiation in combination with VIS (wavelength range 595–1400 nm, intensity 2100 W/m^2) on the retina and cornea in a guinea pig animal model of inclusion conjunctivitis. We investigated the effects 19 days after wIRA/VIS irradiation by comparing a single and double wIRA/VIS treatment with a sham control. By immunolabeling and western blot analyses of critical heat- and stress-responsive proteins, we could not detect wIRA/VIS-induced changes in their expression pattern. Also, immunolabeling of specific retinal marker proteins revealed no changes in their expression pattern caused by the treatment. Our preclinical study suggests wIRA/VIS as a promising and safe therapeutic tool to treat ocular chlamydial infections.

1. Introduction

Trachoma is an ocular disease caused by infection with the bacterium *C. trachomatis* (Ct). Globally, millions of people are affected by ocular Ct infection that, if left untreated, leads to significant visual impairment and irreversible blindness [1,2]. Progression of the disease results in scarring of the conjunctival tissue and inward turning of the eye lid with resulting trichiasis and opacity of the cornea [3]. The commonly used therapy for ocular Ct infection relies on antibiotic treatment with azithromycin, mostly applied *via* mass drug administration in endemic regions [2]. But this treatment has disadvantages in terms of potential antibiotic resistance development and adverse drug reactions [4,5]. Besides, persistent stages of Ct are less susceptible to antibiotic treatment and may result in long-term Ct infection with ongoing chronic inflammatory processes [6,7]. For these reasons, alternative non-chemical treatment options are needed to eliminate trachoma.

Water-filtered infrared A (wIRA), a unique form of heat radiation with deep tissue penetration but a low thermal load on the skin surface, has various clinical applications, like *e.g.* an improvement of acute and chronic wound healing processes [8,9]. Application of wIRA at wavelengths ranging from 780 to 1400 nm has shown to increase the partial oxygen pressure and perfusion of tissues [8]. Furthermore, less pain, reduced inflammation, and lower wound infection frequency have been reported [10,11].

In previous *in vitro* studies, it was demonstrated that exposure of *Chlamydia*-infected Vero, HeLa and human conjunctival epithelial cells (HCjE) to wIRA irradiation caused a significant reduction in chlamydial infectivity [12–14]. Additionally, wIRA treatment did not cause the induction of chlamydial persistence, which represents a developmental stage that is refractory to antibiotic therapy [15]. Irradiation with wIRA combined with visible light (VIS) in the spectrum of 380–780 nm further enhanced these effects [12]. Thus, wIRA/VIS exposure of Ct infected eyes might represent a promising and safe, non-chemical, therapeutic

* Corresponding author.
E-mail address: aleksandra.inic-kanada@meduniwien.ac.at (A. Inic-Kanada).

https://doi.org/10.1016/j.jphotobiol.2021.112306
Received 22 March 2021; Received in revised form 27 August 2021; Accepted 9 September 2021
Available online 10 September 2021

Table 1
List of antibodies used for western blot (WB) and immunolabeling (IL) experiments.

Target of antibody	Company (cat.no.)	Dilution (WB/IL)
Primary antibodies:		
HSP40	Cell signaling (cs-4871)	1:1000/1:100
HSP60	Cell signaling (cs-4870)	1:1000/1:100
HSP70	Cell signaling (cs-4872)	1:1000/1:100
HSP90	Cell signaling (cs-4874)	1:1000/1:100
Akt	Cell signaling (cs-4691)	1:1000/1:100
pAkt	Cell signaling (cs-4060)	1:1000/1:100
Erk1/2	Santa cruz (sc-152)	1:500/1:100
pErk1/2	Cell signaling (cs-4370/ cs9106)	1:1000/1:200
pcRaf	Cell signaling (cs-9421)	1:1000/1:100
pPTEN	Cell signaling (cs-9551)	1:1000/1:100
SAPK/JNK	Cell signaling (cs-9252)	−/1:150
pSAPK/JNK	Cell signaling (cs-4668)	−/1:100
NF-κB	Cell signaling (cs-8242)	−/1:100
pNF-κB	Cell signaling (cs-3036)	−/1:100
Glutamine synthetase	BD Bioscience 10,517	−/1:300
Chx10	Santa cruz (sc365519)	−/1:150
Pax6	DSHB	−/1:100
Sox9	Abcam (ab 5535)	−/1:100
Vinculin	Abcam (ab129002)	1:5000/1:100
Secondary antibodies:		
Rabbit IgG (labeled byAlexa Fluor 594)	Invitrogen A11012	−/1:400
Mouse IgG (labeled by Alexa Fluor 488)	Invitrogen A11001	−/1:400
Rabbit IgG (labeled by HRP)	Dianova 711–035-152	1:5000/−
Mouse IgG (labeled by HRP)	Dianova 715–035-150	1:5000/−

strategy for treating chlamydial infections.

However, a prerequisite for wIRA/VIS-based therapy of Ct infected eyes is to prove that it is harmless and safe to ocular structures, which include the thermo- and light-sensitive retina and the thermo-sensitive cornea [16–19]. An unrestricted functionality of the latter structures is required for vision. Thus, side effects like hyperthermia- or light-induced stress responses in the ocular tissues due to photothermal and photochemical reactions to wIRA/VIS treatment must be precluded.

In the present study, we examined the effects of wIRA irradiation in combination with partially filtered VIS (595–1400 nm) on the retina and cornea of guinea pigs, an established animal model for trachoma-like disease [20]. While we previously demonstrated short- and long-term effects in reducing chlamydial infection (measured by the reduction of the chlamydial load and inflammatory responses), here we focused on the long-term risk assessment of wIRA/VIS on the retina and cornea 19 days after irradiation [21]. To mimic the treatment protocol, we also compared the effect of single irradiation with sequential treatments consisting of two irradiations at an interval of 2 days. The outcome of these treatments was analyzed by monitoring the cellular and phosphorylation levels of heat shock proteins (HSPs) and protein kinases known to be involved in the regulation of cellular responses to temperature changes, oxidative stress, inflammation, and radiation [22–25]. Furthermore, we used immunolabeling techniques targeting specific retinal cell types to investigate whether wIRA/VIS treatment caused changes in the integrity of the retina structure.

The purpose of the presented follow-up study was to assess the safety of wIRA/VIS by evaluating the effects of irradiation treatment on the retina and cornea in a guinea pig model to evaluate the applicability of this radiation-based therapy against chlamydial ocular infections.

2. Materials and Methods

2.1. Ethics Statement

The experiments were approved by the "Ethics Committee for the Welfare of Experimental Animals" at the Institute of Virology, Vaccines and Sera–Torlak, conformed to the Serbian laws and European regulations on animal welfare (Approval No. 323-07-03902/2017-05), adhered to the Association for Research in Vision and Ophthalmology Statement for the Use of Animals in Ophthalmic and Vision Research, and comply with the ARRIVE guidelines. The guinea pigs were observed daily by animal care staff. Terminal euthanasia was carried out by lethal CO_2 overdose.

2.2. Experimental Animals

Female Hartley strain guinea pigs weighing 300–350 g and six weeks of age were used in this experiment. Animals were housed individually in cages with filter tops, given food and water *ad libitum*, and kept on a 12-h light/12-h dark cycle. The guinea pigs were pre-screened for absence of *Chlamydia caviae*-specific antibodies by in-house optimized enzyme-linked immunosorbent assay (ELISA) as previously described [26].

2.3. wIRA Irradiation, Isolation, and Preparation of Guinea Pig Eyes

Bilateral irradiation with wIRA/VIS was performed under anesthesia given intraperitoneally with a mixture of ketamine (30 mg/kg) and xylazine (2 mg/kg). The irradiation with a wIRA radiator, equipped with a BTE 595 filter (Hydrosun 750, Hydrosun GmbH, Müllheim, Germany), was carried out with a radiation spectrum ranging from 595 nm up to 1400 nm and an irradiation dose of 2100 W/m^2. We had three groups in the experiment:

1) Animals received either a single irradiation for 30 min (wIRA/VIS 1×, $n = 3$).
2) Animals received two radiation treatments of 30 min each in 2 days interval (wIRA/VIS 2×, n = 3).
3) Non-irradiated animals were used as controls (no wIRA/VIS, n = 3).

During the irradiation, temperature probes were inserted between the conjunctiva and the cornea to measure the temperature during wIRA/VIS treatment. Recorded physiological temperatures at the corneal surface ranged between 37.5 and 37.8 °C in all animals.

2.4. Post-Mortem Investigations

On day 19 after the first irradiation, the guinea pigs were euthanized, and their eye bulbs were isolated. According to standard immunohistochemistry procedures, one eye per animal was fixed 24 h in 4% buffered paraformaldehyde for paraffin embedding. The other eye was placed in liquid nitrogen and stored at −80 °C for protein analyses by western blotting.

2.5. Immunolabeling

Paraffin sections (6 μm) of formalin-fixed eye bulbs were dewaxed in xylene and rehydrated through graded ethanol to water (immunolabeling protocol modified from [27]). Antigen retrieval was performed by heat-induced epitope demasking (citrate buffer, pH 6.0, 98 °C for 1 h. Primary antibodies (see Table 1) were incubated over night at room temperature in 0.2% TritonX/PBS, washed three times with 0.1% Tween 20/PBS, and subsequently incubated with the secondary antibody (see Table 1) for 1.5 h at room temperature in the dark. After three washes with 0.1% Tween 20/PBS, DAPI staining was performed for 10 min (0.2 mg/ml DAPI/ PBS; Sigma Aldrich, Germany). Sections were mounted on glass slides using mounting medium (Ibidi, Gräfelfing, Germany) and sealed with nail polish. As negative controls, the primary antibody was omitted.

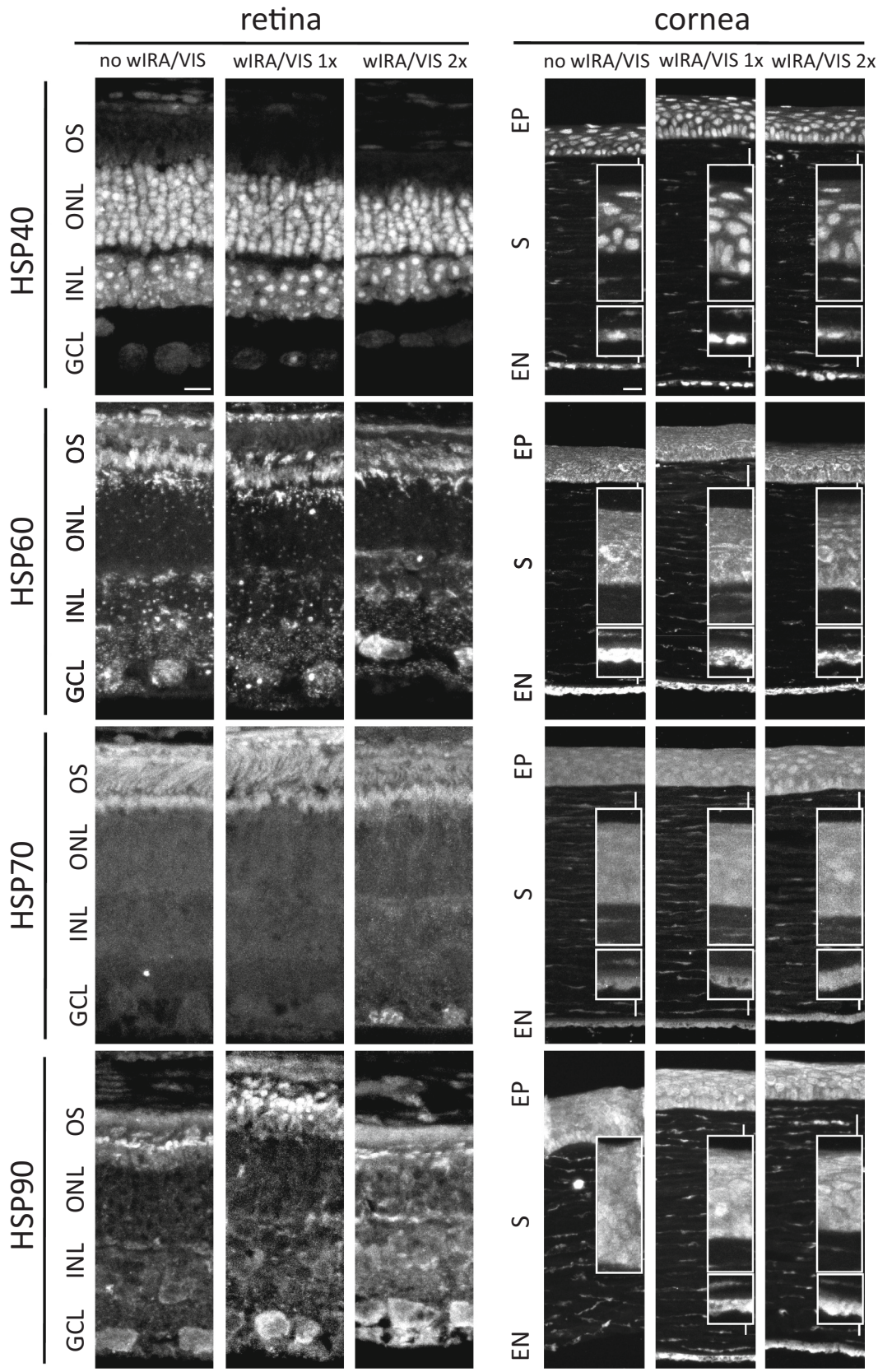

Fig. 1. Localization of HSPs in the guinea pig retina and cornea 19 days after wIRA/VIS treatment. Immunolabeling of HSP40, HSP60, HSP70, and HSP90 in retinal layers (OS-outer segments, ONL-outer nuclear layer, INL-inner nuclear layer, and GCL-ganglion cell layer) and corneal layers (EP-epithelium, S-Stroma, and EN-endothelium). Comparison of non-irradiated (no wIRA/VIS) tissues with ones subjected to single (wIRA/VIS 1×) or sequential (wIRA/VIS 2×) irradiation. Inserts in cornea images show magnified sections of EP and EN. Scale bars = 10 μm retina, 20 μm cornea.

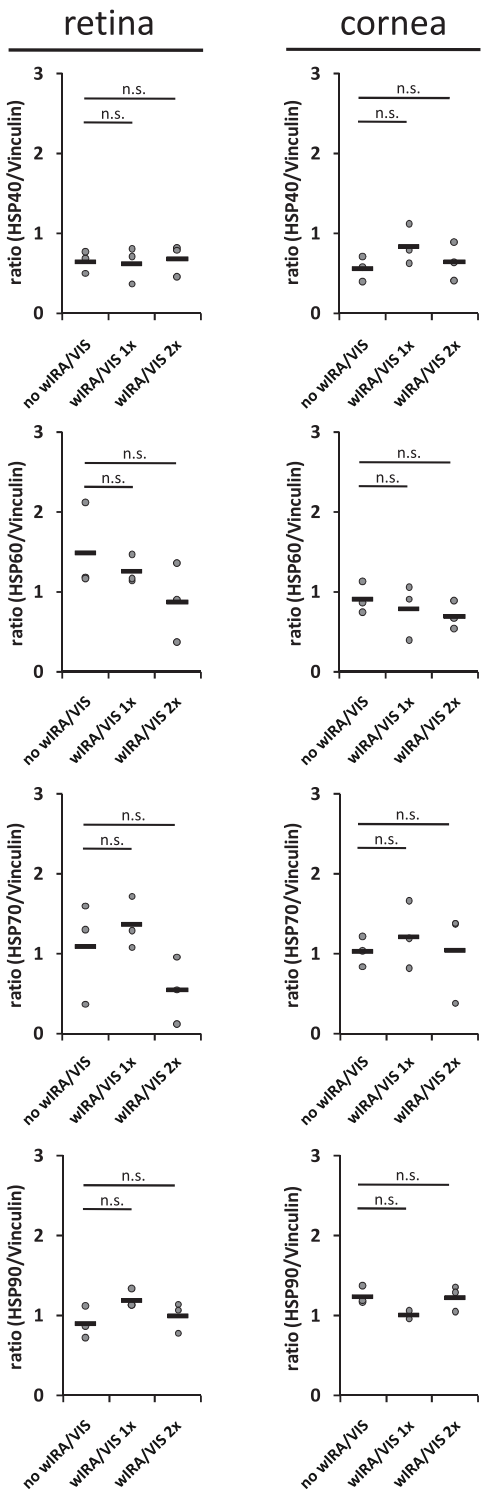

Fig. 2. Expression of HSPs in the guinea pig retina and cornea 19 days after wIRA/VIS treatment. Quantitative western blot analyses of HSP40, HSP60, HSP70, and HSP90 in the retina and cornea. Comparison of non-irradiated (no wIRA/VIS) tissues with ones subjected to single (wIRA/VIS 1×) or sequential (wIRA/VIS 2×) irradiation. For quantification, the data were normalized to the content of the constitutively expressed protein vinculin (ratio). Data are depicted as means (bars) of single values (points) for each animal ($n = 3$ per group). Statistical significance was evaluated using a one-way ANOVA, followed by post-hoc (Dunnett) test (P values <0.05 were considered significant). n.s. = not significant.

Table 2
Localization of immunolabeled HSPs in the retina and cornea.

	Retina	Cornea
HSP40 *(heat shock protein40)*	-In nuclei (strongest in hetero-chromatic regions)	-In nuclei (pan-nuclear)
HSP60 *(heatshockprotein60)*	-In cytoplasm (dot-shaped) - additional in OS and GCL	-Predominant in cytoplasm
HSP70 *(heatshockprotein70)*	-Faint signals (slightly stronger in OS)	-In nuclei and cytoplasm (slightly stronger in nuclei)
HSP90 *(heatshockprotein90)*	-Predominant in cytoplasm (strongest in OS and GCL)	-Predominant in nuclei

2.6. Microscopy and Imaging

Images of the tissues were taken on a confocal microscope (Leica TCS SP5 II, Leica Microsystems CMS GmbH, Mannheim, Germany) with LAS AF Lite software (Leica) at a magnification of 630 x for retina sections and magnification of 400 x for cornea sections. Parameters for all images were a maximum intensity projection of image stacks ($z = 15$) with a focus plane distance of 700 nm. The images were arranged using ImageJ software.

2.7. Western Blotting

For western blotting, frozen eye bulbs from guinea pigs were dissected while thawing, and tissue samples (retina, cornea) were isolated separately. Tissues were sonicated two times for 30 s each in 1 x cell lysis buffer (Cell signaling) with 1× protease inhibitor Complete® and 1 x PhosphoStop (Roche) (western blot protocol modified from [27]). After centrifugation of the cell extracts for 15 min (15,700 g) at 4 °C, the protein concentration was determined. The cell lysates were boiled with SDS Laemmli loading buffer [4% (*w/v*) SDS, 200 mM DTT, 120 mM Tris/HCl, 10 mMβ-mercaptoethanol, 20% (*v*/v) glycerin, 0.02% bromophenol blue, pH 6.8] for 8 min at 95 °C. Proteins were separated *via* 10% SDS–PAGE and transferred to a PVDF membrane. The membrane was incubated with primary antibodies (see Table 1) in 5% low-fat milk or 5% BSA in TBS/0.1% Tween-20 over night at 4 °C, followed by addition of the HRP-conjugated secondary antibody (see Table 1) in 2.5% low-fat milk in 0.1% Tween-20/TBS for 1 h. The immunoblots were developed using Western Bright Chemilumineszenz Substrat Quantum (Biozyme). Signal detection was carried out with a ChemiDoc gel imaging system (BioRad) and the ImageLab software. For the quantification of detection signals, ImageJ software was used.

2.8. Statistics

For quantification of the investigated proteins, western blot data were normalized to Vinculin content (giving a protein/Vinculin ratio) and depicted as mean (bars) of single values (points) for each animal ($n = 3$ per group). Statistical analysis was performed using R Studio [28]. Protein ratios for each animal and group were imported for one-way analysis of variance (ANOVA) to test for statistical significance, followed by post-hoc analysis (Dunnett) and model diagnostics. A probability (P) value of 0.05 was set as the significance threshold.

3. Results and Discussion

Our study aimed to assess potential heat- or light-induced effects of wIRA radiation in combination with VIS (wavelength range 595–1400 nm) on the retina and cornea of guinea pigs. This investigation is important since light as a form of electromagnetic radiation could potentially be harmful *via* photothermal and photochemical reactions, depending on the exposure time and light energy [17].

This study is a follow-up to our previous study where we showed that wIRA/VIS can efficiently combat chlamydial infection [21]. There are

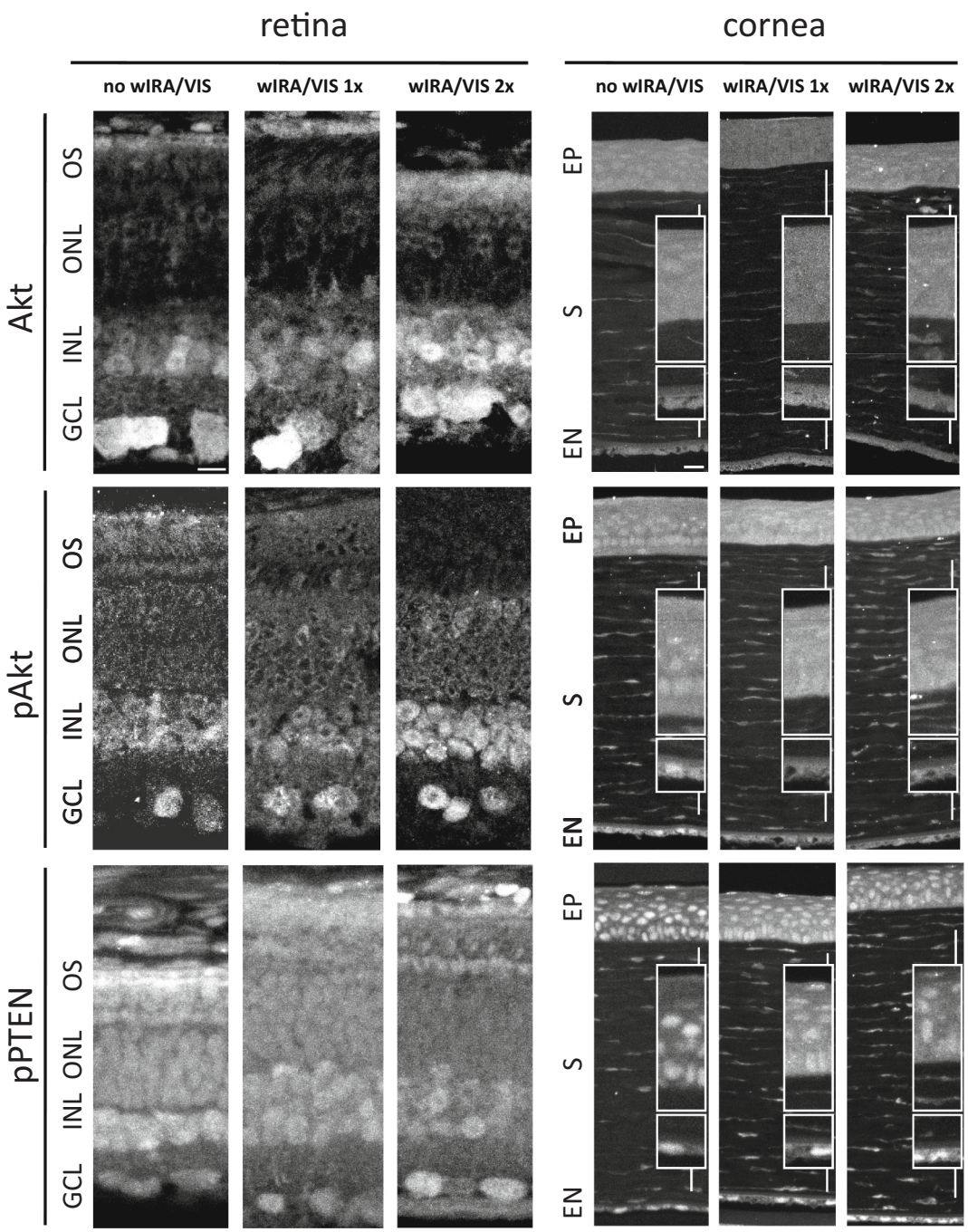

Fig. 3. Localization of Akt, pAkt, and pPTEN in the guinea pig retina and cornea 19 days after wIRA/VIS treatment. Immunolabeling of Akt, pAkt, and pPTEN in retinal layers (OS-outer segments, ONL-outer nuclear layer, INL-inner nuclear layer, and GCL-ganglion cell layer) and corneal layers (EP-epithelium, S-Stroma, and EN-endothelium). Comparison of non-irradiated (no wIRA/VIS) tissues with ones subjected to single (wIRA/VIS 1×) or sequential (wIRA/VIS 2×) irradiation. Inserts in cornea images show magnified sections of EP and EN. Scale bars = 10 μm retina, 20 μm cornea.

only two animal models available that satisfyingly mimic ocular chlamydial infection in humans: non-human primates (NHP) and guinea pigs. NHP research is coupled with ethical concerns and very high costs linked with these experiments. This is one of the reasons why we use the guinea pig model of inclusion conjunctivitis, where animals are infected with *Chlamydia caviae* [21,29–33]. The model's main advantage is that changes in the conjunctiva of individual animals throughout infection can easily be assessed by gross pathology and can be correlated to the number of bacteria isolated from ocular swabs. The size of guinea pigs allows histopathologic and gene expression studies on conjunctival tissue originating from one animal [34]. Our previous study was investigating female guinea pigs [21]; in future studies, inclusion of male guinea pigs is recommended to further corroborate our findings.

wIRA (780–1400 nm) and VIS (400–780 nm) passes the transparent ocular structures (cornea, lens, and vitreous body) to the ocular fundus [35]. The retina in the ocular fundus converts stimuli of VIS into nerve signals and is thus one of the most important tissue for the visual capacity. Infrared (IR) A is not absorbed by the retina, but by the adjacent retinal pigment epithelium (RPE). Consequently, photothermal damage of retinal cells occur by indirect heating [36]. Since guinea pigs (Hartley strain) usually lack or have much less pigmentation of the RPE compared to humans, wIRA absorption and consequently heat generation could be

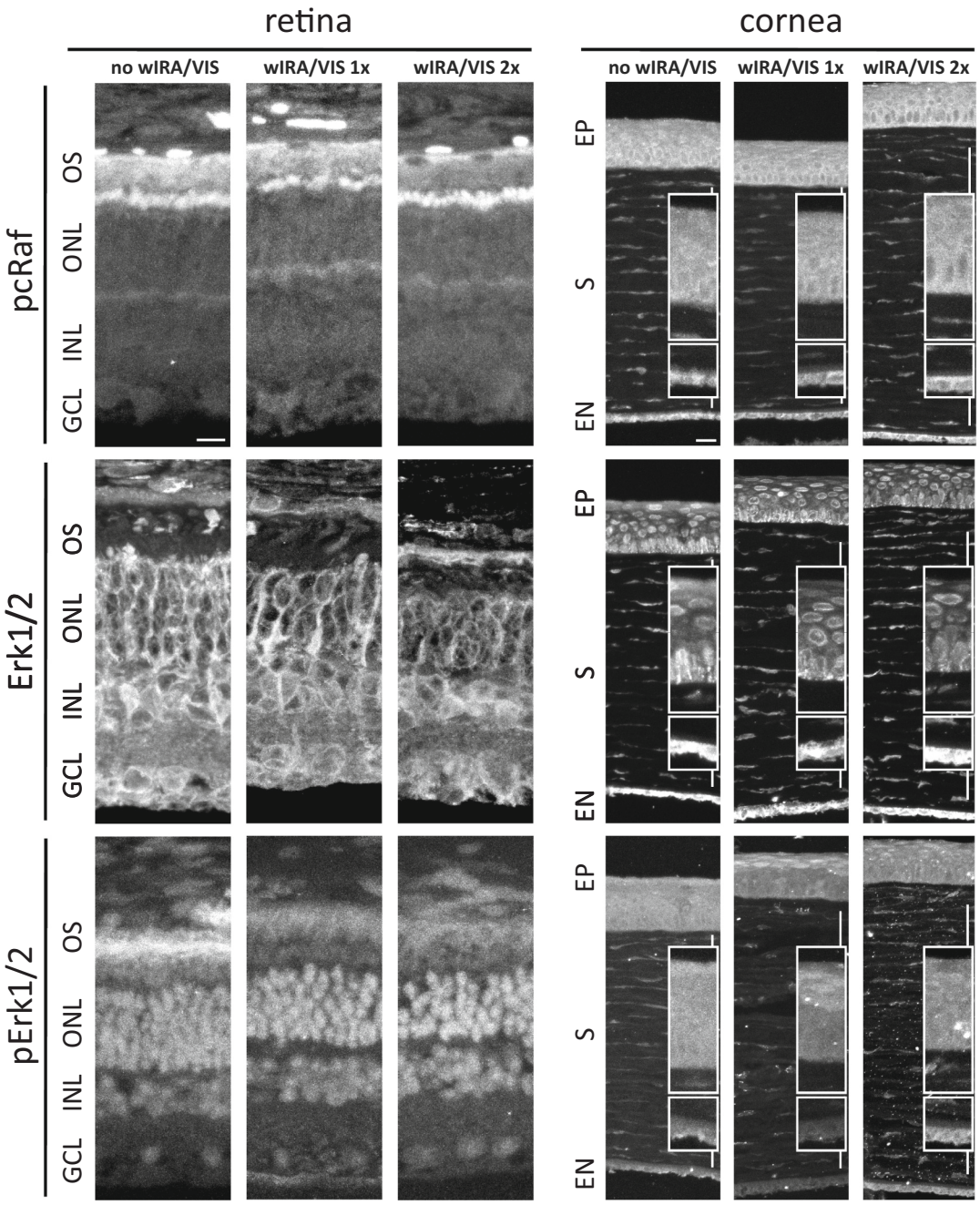

Fig. 4. Localization of pcRaf, Erk1/2and pErk1/2 in the guinea pig retina and cornea 19 days after wIRA/VIS treatment. Immunolabeling of pcRaf, Erk1/2, and pErk1/2 in retinal layers (OS-outer segments, ONL-outer nuclear layer, INL-inner nuclear layer, and GCL-ganglion cell layer) and corneal layers (EP-epithelium, S-Stroma, and EN-endothelium). Comparison of non-irradiated (no wIRA/VIS) tissues with ones subjected to single (wIRA/VIS 1×) or sequential (wIRA/VIS 2×) irradiation. Inserts in cornea images show magnified sections of EP and EN. Scale bars = 10 μm retina, 20 μm cornea.

less pronounced. With regards to the threshold of a non-critical temperature increase, a rise of 10 °C above the body temperature will produce permanent retina damage by simple denaturation of proteins [17]. However, even thermal effects significantly below this limit are capable to alter gene expression in the retina and adjacent RPE, and therefore entail the risk of a long-term damage to the tissues [37,38]. Even if the cornea transmits most of the IRA, absorption by neighboring ocular structures (lens and iris) could possibly contribute to a wIRA-induced heat accumulation in the eye affecting the cornea by indirect heating and thus could lead to photothermal damage. The lens is another heat-sensitive ocular structure and demands investigation in future studies, as it is known to be sensitive to infrared, exemplified by cataract formation after high IR exposure [36,39]. In this study, we performed investigations on photothermal and photochemical effects of wIRA/VIS on the retina and cornea of guinea pigs to assess preliminary safety aspects of wIRA/VIS as a treatment option against chlamydial infections of the eye.

3.1. *wIRA/VIS and Temperature Measurements*

Our previous *ex vivo* study shows, that upon irradiation of unprotected isolated pig eyes, the corneal (35 °C) and vitreal (37.6 °C) temperature remained near the physiological values of the cornea (34–35 °C) and the vitreous body (33.9 °C) of humans, and the vitreous body of pigs (34.7–35.8 °C) [13,40–42]. During *in vivo* ocular irradiation of guinea pigs with the same wIRA/VIS irradiance (2100 W/m^2), we

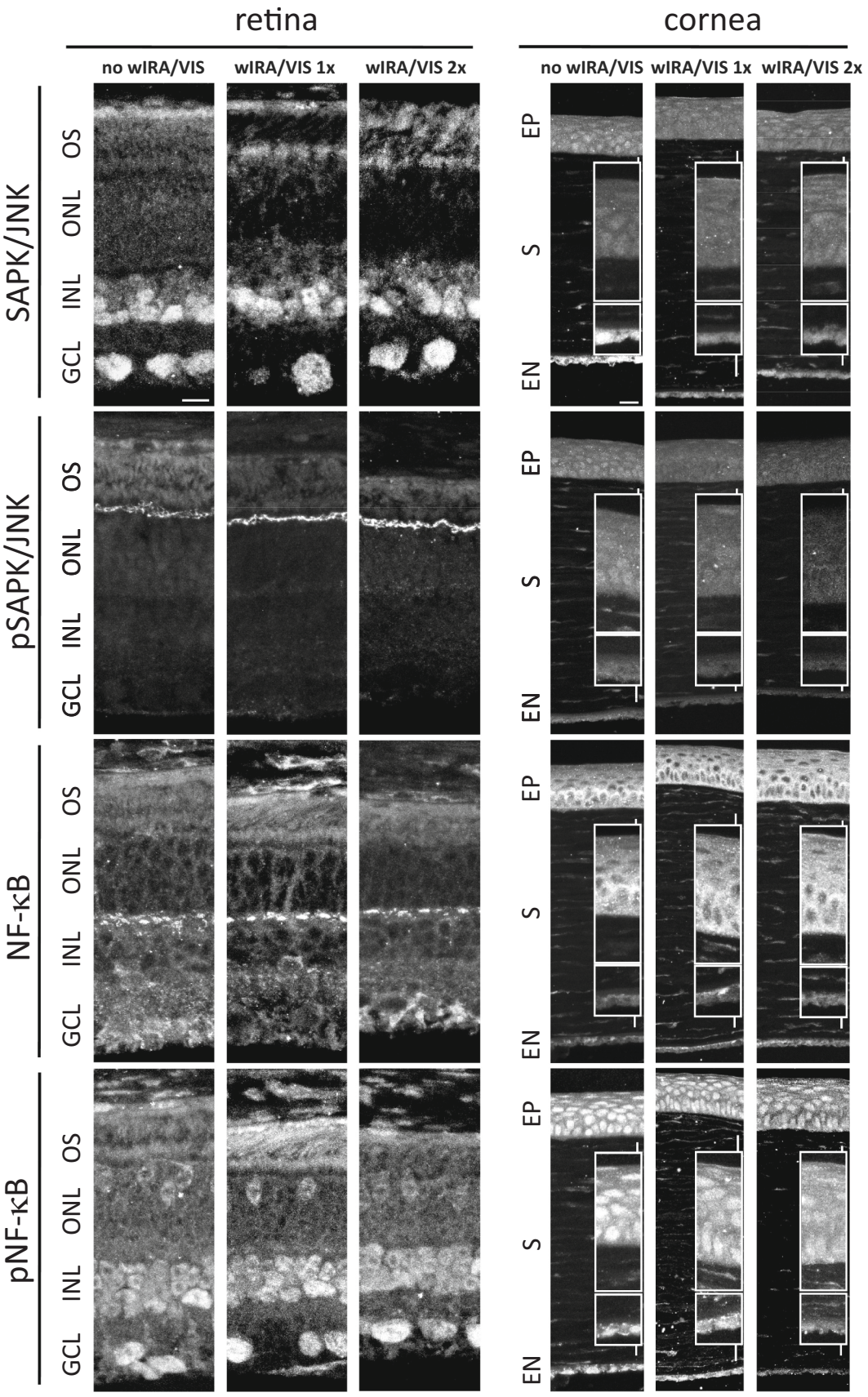

Fig. 5. Localization of SAPK/JNK, pSAPK/JNK, NF-κB and pNF-κBin the guinea pig retina and cornea 19days after wIRA/VIS treatment. Immunolabeling of SAPK/JNK, pSAPK/JNK,NF-κB, and pNF-κB in retinal layers (OS-outer segments, ONL-outer nuclear layer, INL-inner nuclear layer, and GCL-ganglion cell layer) and corneal layers (EP-epithelium, S-Stroma, and EN-endothelium). Comparison of non-irradiated (no wIRA/VIS) tissues with ones subjected to single (wIRA/VIS 1×) or sequential (wIRA/VIS 2×) irradiation. Inserts in cornea images show magnified sections of EP and EN. Scale bars=10μm retina, 20μm cornea.

Table 3
Localization of immunolabeled stress-responsive proteins in the retina and cornea.

	Retina	Cornea
Akt *(v-akt murine thymoma viral oncogene homolog)*	-Predominant in nuclei in the INL and GCL, and some nuclei in ONL (weaker in heterochromatic regions)	-In nuclei and cytoplasm (slightly stronger in nuclei)
pAkt *(phosphorylated Akt)*	-Predominant in nuclei in the INL, GCL, and ONL (weaker in heterochromatic regions)	
pPTEN *(phosphorylated phosphatase and tensin homolog)*	-In nuclei and cytoplasm (slightly stronger in nuclei)	-Predominant in nuclei
• antagonist of Akt		
pcRaf *(phosphorylated rapidly accelerated fibrosarcoma or rat fibrosarcoma)*	-Faint signals (strong in OS)	-In nuclei and cytoplasm (slightly stronger in cytoplasm)
• part of the Erk1/2 pathway		
Erk1/2 *(extracellular signal-regulated kinase)*	-Predominant in cytoplasm (and cellular processes)	-Predominant in nuclei (especially in the peri-nuclear regions in the EP)
pErk1/2 *(phosphorylated Erk1/2)*	-Predominant in nuclei	-In nuclei and cytoplasm (evenly distribution)
SAPK/JNK *(stress-activated protein kinase, c-Jun N-terminal kinase)*	-Predominant in nuclei in the GCL and the lower INL	-In nuclei and cytoplasm (slightly stronger in nuclei)
pSAPK/JNK *(phosphorylated SAPK/JNK)*	-Faint signals (strong between the ONL and OS)	
NF-κB *(nuclear factor-kappa B)*	-Predominant in cytoplasm (strong between ONL and INL)	-Predominant in cytoplasm
pNF-κB *(phosphorylated NF-κB)*	-Predominant in nuclei (weaker in heterochromatic regions)	-Predominant in nuclei

assessed the temperature on top of the cornea and measured a maximum of 37.8 °C. However, this value is well below the temperature, which causes cellular stress responses [43,44]. The higher corneal temperature measured *in vivo* (37.8 °C) compared to *ex vivo* (35 °C) experiments could be due to an accumulation of heat in the anterior eye chamber, since eyelids were closed, covering the cornea, and eyeballs were surrounded by adjacent tissues. Consequently, the cooling effect normally caused by the lid stroke is absent and heat dissipation is limited by the surrounding tissue.

Nevertheless, these data suggest that wIRA/VIS treatment does not increase the temperature in the retina and cornea towards a hazardous limit, but the exact temperature increase during *in vivo* irradiation in the interior ocular structures could not be assessed technically and therefore remains unclear.

3.2. wIRA/VIS and Heat-Responsive Proteins

Since the temperature measurements do not rule out photothermal effects, we used an indirect assay by measuring the impact of wIRA/VIS treatment on expression levels of heat shock proteins (HSPs) in the retina and cornea. It is well established that HSPs are upregulated after stressful stimuli such as heat, oxidative stress, or irradiation and are responsible for the stabilization of cellular proteins to protect them from denaturation and regulation of cell death processes [22,45]. An upregulation of HSPs has already been shown in ocular structures after hyperthermia, IR-, and UV radiation, and also in processes controlling protection and wound healing [46–49].

To evaluate HSPs localization differences 19 days after wIRA/VIS treatment, immunolabeling for HSP40, HSP60, HSP70, and HSP90 was carried out in the retina and cornea (Fig. 1). For an illustrated overview of the nuclear layers of the retina (ONL-outer nuclear layer, INL-inner nuclear layer, GCL-ganglion cell layer) and layers of the cornea (EP-epithelium, S-stroma, EN-endothelium), DAPI staining was performed (Fig. S1). Throughout the layers of the tissues, all HSPs revealed a specific localization pattern in non-irradiated tissues (no wIRA/VIS, see Table 2), which was not affected by either single (wIRA/VIS 1×) or sequential (wIRA/VIS 2×) treatment.

To confirm the observations of the immunolabeling analyses, we further checked the quantitative expression of HSPs by western blot analyses and compared protein levels of retinal and corneal tissues (Fig. 2, exemplary western blots shown in Fig. S2). For quantification, the data were normalized to the levels of the constitutively expressed protein vinculin, which also showed no differences between non- and irradiated samples by immunolabeling (Fig. S3). Western blot analyses of the HSP expression in the retina and cornea showed only mild variations in the mean values of non-irradiated (no wIRA/VIS) and irradiated (wIRA/VIS 1×, wIRA/VIS 2×) tissues, and these differences were not significant.

In summary, these results are consistent with the temperature measurements, which have already ruled out an excessive temperature increase during wIRA/VIS irradiation at least on the cornea. The presented data furthermore underpin that there is no evidence for long-term activation of HSPs in retinal or corneal tissue, even if regulation shortly after wIRA/VIS irradiation cannot be excluded. This means that either the temperature inside the eye never exceeded a critical value or that the heat does not accumulate but is well dissipated by the choroidea's blood flow in the ocular fundus [50]. Furthermore, wIRA/VIS treatment does not lead to an activation of HSPs by non-thermal effects shown to be induced in response to environmental and chemical stress (oxidation, inflammation, toxins) [22].

3.3. wIRA/VIS and Stress-Responsive Proteins

In addition to the thermal component, wIRA is known to have additional photochemical effects that are thought to be caused by photon absorption by cytochrome *c* oxidase (COX) in the mitochondrial membrane [51]. This reaction generates reactive oxygen species (ROS) that are released into the cytoplasm, where they trigger cellular stress-mediated signaling pathways through various protein kinases (*e.g.* mitogen-activated protein kinases (MAPKs)) and transcription factors (like nuclear factor-kappa B (NF-κB)) [52]. In ocular structures, these proteins are known to regulate processes such as inflammation, apoptosis, proliferation, corneal wound healing, and retinal neovascularization [53,54].

As representatives for stress-responsive proteins, we investigated the proteins Akt, pAkt, and pPTEN (Fig. 3), pcRaf, Erk1/2, and pErk1/2 (Fig. 4), SAPK/JNK, NF-κB, and pNF-κB (Fig. 5) in the retina and cornea by immunolabeling 19 days after wIRA/VIS treatment. All stress-responsive proteins revealed a specific localization pattern in non-irradiated tissues (no wIRA/VIS, see Table 3), which is not affected by either single (wIRA/VIS 1×) or sequential (wIRA/VIS 2×) irradiations.

In line with these findings, quantitative western blot analyses of retinal and corneal tissues did not reveal any significant differences in the expression of Akt, pAkt, pPTEN, pcRaf, Erk1/2, and pErk1/2after wIRA/VIS irradiation (Fig. 6, exemplary western blots shown in Fig. S4).

In summary, we could not observe wIRA/VIS-induced long-term changes in the expression levels of critical stress-responsive proteins in the retina and cornea of guinea pigs, even if regulation shortly after wIRA/VIS irradiation cannot be excluded. It must be mentioned that the expression of COX in the mitochondria is thought to be downregulated in the retinal cells of guinea pigs [55]. Consequently, it is conceivable

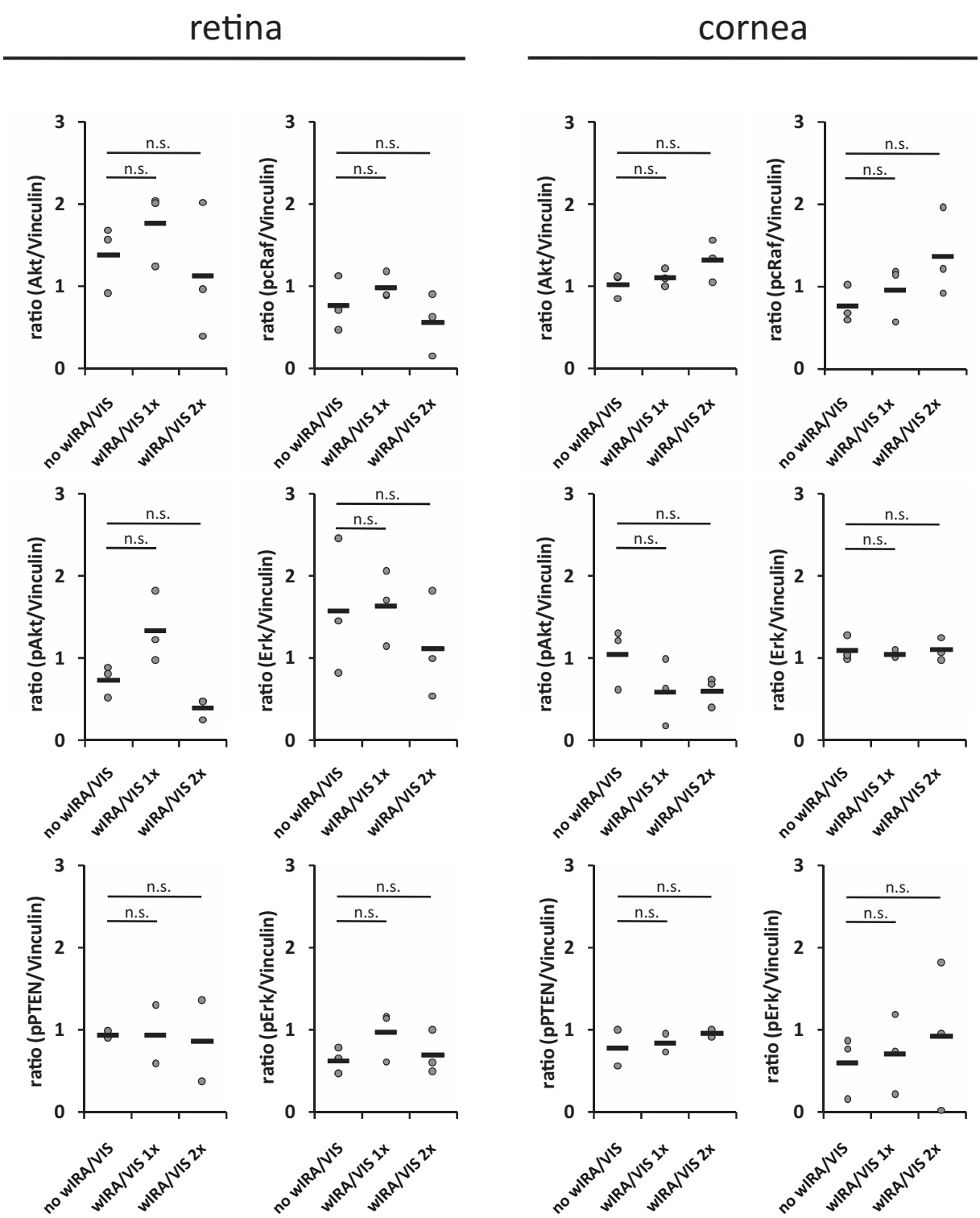

Fig. 6. Expression of stress-responsive proteins in the guinea pig retina and cornea 19 days after wIRA/VIS treatment. Quantitative western blot analyses of Akt, pAkt, pPTEN, pcRaf, Erk1/2, and pErk1/2 in the retina and cornea. Comparison of non-irradiated (no wIRA/VIS) tissues with ones subjected to single (wIRA/VIS 1×) or sequential (wIRA/VIS 2×) irradiation. For quantification, the data were normalized to the content of the constitutively expressed protein vinculin (ratio). Data are depicted as means (bars) of single values (points) for each animal ($n = 3$ per group). Statistical significance was evaluated using a one-way ANOVA, followed by post-hoc (Dunnett) test (P values <0.05 were considered significant). n.s. = not significant.

that less ROS would be generated by irradiation treatment, which in turn would activate comparatively less stress reactions. However, in our previous studies, we did not find any induction of stress-regulating proteins (p38, Akt, Erk or SAPK/JNK) in retinal explants of mice at shorter time points after 1000 W/m^2 wIRA irradiation [13]. Moreover, HeLa cells exhibited no changes in their stress proteins directly after irradiation with a higher dose of 3700 W/m [12].

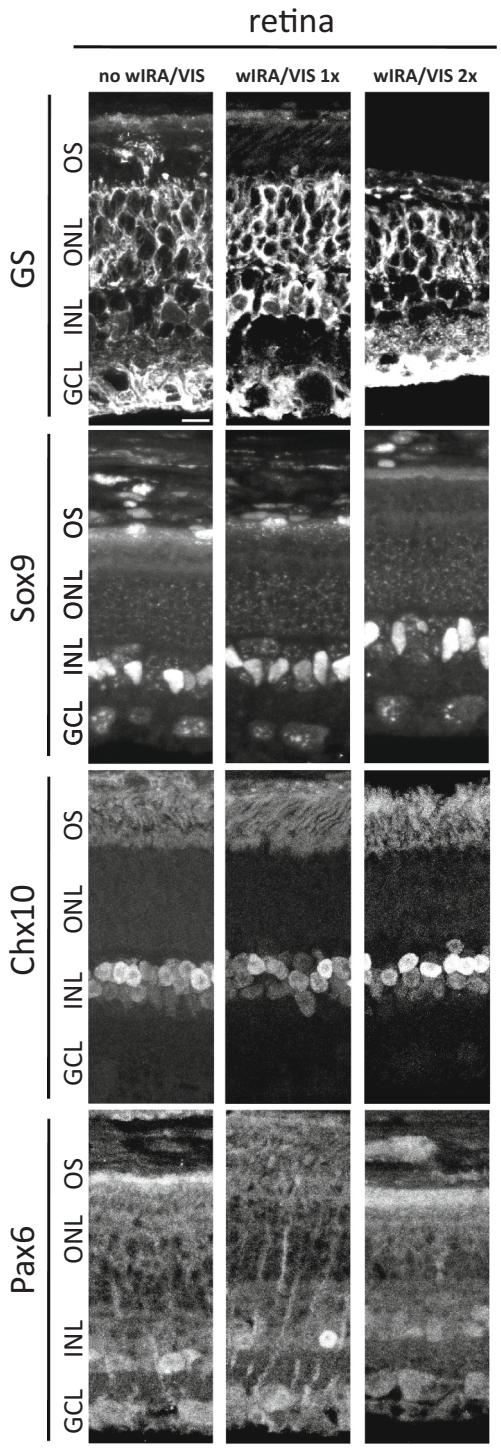

Fig. 7. Localization of cell type-specific marker proteins in the guinea pig retina 19 days after wIRA/VIS treatment. Immunolabeling of glutamine synthetase (GS) and the transcription factors Sox9, Chx10, and Pax6 in retinal layers (OS-outer segments, ONL-outer nuclear layer, INL-inner nuclear layer, and GCL-ganglion cell layer). Comparison of non-irradiated (no wIRA/VIS) tissues with ones subjected to single (wIRA/VIS 1×) or sequential (wIRA/VIS 2×) irradiation. Scale bar = 10 µm.

3.4. wIRA/VIS and the Retina Structure

Previous results did not show any evidence for a wIRA/VIS-mediated response in critical heat- or stress-induced proteins. The experimental design in which the parameters of interest are monitored 19 days after irradiation leaves the possibility that a potentially harmful effect might occur at earlier time points. To examine these early effects, we took a closer look at the retina, which is known to be the most light-sensitive part of the eye. In the retina, light is absorbed by chromophores located in photoreceptors, ganglion-, and Müller glial cells, as well as in cells of the adjacent RPE [56]. For near IR radiation (670 nm), some beneficial effects, including improvement of mitochondrial function and reduced inflammation in the aged retina are already described [57]. In contrast, the absorption of blue light (400–500 nm) by the retina can be hazardous; it might trigger apoptotic cell death in photoreceptors and RPE cells resulting in impaired vision [35,58].

Hence, we assessed the impact of wIRA/VIS (595–1400 nm) on the survival and the morphology of specific cell types in the retina to investigate whether this treatment might induce changes as a long-term consequence. To analyze the integrity of the retinal structure 19 days after single (wIRA/VIS 1×) or sequential (wIRA/VIS 2×) irradiation treatment, we examined cell type-specific marker proteins (glutamine synthetase, Sox9, Chx10 and Pax6) by immunolabeling methods (Fig. 7).

As a first step, we analyzed Müller glia cells as the central glia cells of the retina. Their primary metabolic function confers neuroprotection to the retina resulting in the promotion of neural cell repair and survival [59]. Labeling against the glutamine synthetase, a specific marker of Müller glia cells, revealed that they are spatially distributed along the retina, facilitating their close membrane interactions with all retinal neurons. Nuclei of Müller glia cells are located in the inner nuclear layer (INL), as shown by labeling targeting Sox9 and partially Chx10. The transcription factor Sox9 additionally showed a dot-shaped pattern in all other nuclei of the retina. To further check the impact of wIRA/VIS on bipolar cells in the INL, responsible for signal transduction between photoreceptor cells in the outer nuclear layer (ONL) and the ganglion cells in the ganglion cell layer (GCL), labeling against the bipolar cell marker Chx10 was performed. Chx10 showed strong signals in the nuclei, predominantly in euchromatic regions of bipolar cells and in a subset of Müller glia cells. Finally, we checked the expression of the transcription factor Pax6, allowing us to detect amacrine cells in the basal part of the INL and the ganglion cells in the GCL.

Our data show that neither single (wIRA/VIS 1×) nor sequential (wIRA/VIS 2×) irradiation caused any changes in the specific expression patterns of glutamine synthetase, Sox9, Chx10, and Pax6 compared to the non-irradiated (no wIRA) retina. Consequently, wIRA/VIS treatment did not affect the abundance and the general morphology of retinal cells, which implies that wIRA/VIS treatment does not trigger degenerative processes in the retina. In contrast, the absorption of blue light (400–500 nm) by the retina can be hazardous; it might trigger apoptotic cell death in photoreceptors and RPE cells resulting in impaired vision [35,58] and theoretically could serve as positive control for retinal damage investigations. In our study, however, we focused on the effects of wIRA/VIS in order to assess this treatment's safety profile in terms of stress kinases and HSPs, the factors that are most likely changed upon heat irradiation.

4. Conclusion

In the present study, we provide preliminary evidence on wIRA/VIS-based therapy's impact on the retina and the cornea in a guinea pig model *in vivo*. We monitored a spectrum of relevant heat- and stress-responsive proteins and did not observe any wIRA/VIS-induced activation or long-term changes 19 days after irradiation. Furthermore, cell-specific marker proteins' immunolabeling revealed no changes in the abundance or morphology of retinal cells as a long-term consequence due to wIRA/VIS treatment. As our first study demonstrated wIRA/VIS efficacy to treat chlamydial ocular infections *in vivo*, this study now confirms wIRA/VIS as a new non-chemical treatment device in a pre-clinical animal model excluding adverse side effects. Nevertheless, the effects of wIRA/VIS on ocular structures need to be investigated in more detail and must be optimized for clinical application in humans in the

future.

Supplementary data to this article can be found online at https://doi.org/10.1016/j.jphotobiol.2021.112306.

Declaration of Competing Interest

The authors declare that they have no known competing financial interests or personal relationships that could have appeared to influence the work reported in this paper.

Acknowledgement

This work was supported by the Dr. med. h.c. Erwin Braun Foundation, Basel, Switzerland. We thank Radmila Miljkovic, Ana Filipovic and Bozidar Jokanovic for technical help.

References

[1] G. Satpathy, H.S. Behera, N.H. Ahmed, Chlamydial eye infections: current perspectives, Indian J. Ophthalmol. 65 (2017) 97–102.
[2] WHO, Report of the 18th meeting of the W.H.O Alliance for the Global elimination of Trachoma by 2020, World Heal. Organ, 2014.
[3] H.R. Taylor, M.J. Burton, D. Haddad, S. West, H. Wright, Trachoma, Lancet 384 (2014) 2142–2152.
[4] J.R. Evans, A.W. Solomon, R. Kumar, Á. Perez, B.P. Singh, R.M. Srivastava, E. Harding-Esch, Antibiotics for trachoma, Cochrane Database Syst. Rev. 9 (2019) Cd001860.
[5] T. Mestrovic, S. Ljubin-Sternak, Molecular mechanisms of *Chlamydia trachomatis* resistance to antimicrobial drugs, Front. Biosci. (Landmark Ed) 23 (2018) 656–670.
[6] N. Borel, A.M. Sauer-Durand, M. Hartel, J. Kuratli, P. Vaupel, N. Scherr, G. Pluschke, wIRA: hyperthermia as a treatment option for intracellular bacteria, with special focus on Chlamydiae and mycobacteria, Int. J. Hyperth. 37 (2020) 373–383.
[7] N. Somboonna, N. Ziklo, T.E. Ferrin, J. Hyuk Suh, D. Dean, Clinical persistence of *Chlamydia trachomatis* sexually transmitted strains involves novel mutations in the functional αββα tetramer of the tryptophan synthase operon, mBio (2019) 10.
[8] G. Hoffmann, M. Hartel, J.B. Mercer, Heat for wounds - water-filtered infrared-A (wIRA) for wound healing - a review, Ger. Med. Sci. 14 (2016) Doc08.
[9] J. Kuratli, N. Borel, Perspective: water-filtered infrared-A-radiation (wIRA) - novel treatment options for chlamydial infections? Front. Microbiol. 10 (2019) 1053.
[10] M. Hartel, P. Illing, J.B. Mercer, J. Lademann, G. Daeschlein, G. Hoffmann, Therapy of acute wounds with water-filtered infrared-A (wIRA), GMS Krankenhhyg Interdiszip 2 (2007) Doc53.
[11] B.M. Künzli, F. Liebl, P. Nuhn, T. Schuster, H. Friess, M. Hartel, Impact of preoperative local water-filtered infrared A irradiation on postoperative wound healing: a randomized patient- and observer-blinded controlled clinical trial, Ann. Surg. 258 (2013) 887–894.
[12] H. Marti, M. Koschwanez, T. Pesch, C. Blenn, N. Borel, Water-filtered infrared a irradiation in combination with visible light inhibits acute chlamydial infection, PLoS One 9 (2014), e102239.
[13] C. Rahn, H. Marti, A. Frohns, F. Frohns, C. Blenn, C.A. Leonard, T. Barisani-Asenbauer, E. Stein, N. Borel, Water-filtered infrared A reduces chlamydial infectivity in vitro without causing ex vivo eye damage in pig and mouse models, J. Photochem. Photobiol. B 165 (2016) 340–350.
[14] J. Kuratli, T. Pesch, H. Marti, C.A. Leonard, C. Blenn, P. Torgerson, N. Borel, Water filtered infrared A and visible light (wIRA/VIS) irradiation reduces *Chlamydia trachomatis* infectivity independent of targeted cytokine inhibition, Front. Microbiol. 9 (2018) 2757.
[15] P.B. Wyrick, *Chlamydia trachomatis* persistence in vitro: an overview, J. Infect. Dis. 201 (Suppl. 2) (2010) S88–S95.
[16] H. Faby, J. Hillenkamp, J. Roider, A. Klettner, Hyperthermia-induced upregulation of vascular endothelial growth factor in retinal pigment epithelial cells is regulated by mitogen-activated protein kinases, Graefes Arch. Clin. Exp. Ophthalmol. 252 (2014) 1737–1745.
[17] P.N. Youssef, N. Sheibani, D.M. Albert, Retinal light toxicity, Eye (Lond) 25 (2011) 1–14.
[18] S. Mergler, M. Valtink, S. Takayoshi, Y. Okada, M. Miyajima, S. Saika, P.S. Reinach, Temperature-sensitive transient receptor potential channels in corneal tissue layers and cells, Ophthalmic Res. 52 (2014) 151–159.
[19] L. Kessel, L. Johnson, H. Arvidsson, M. Larsen, The relationship between body and ambient temperature and corneal temperature, Invest. Ophthalmol. Vis. Sci. 51 (2010) 6593–6597.
[20] S. Phillips, B.L. Quigley, P. Timms, Seventy years of Chlamydia vaccine research - limitations of the past and directions for the future, Front. Microbiol. 10 (2019) 70.
[21] A. Inic-Kanada, M. Stojanovic, R. Miljkovic, E. Stein, A. Filipovic, A. Frohns, N. Zöller, J. Kuratli, T. Barisani-Asenbauer, N. Borel, Water-filtered infrared A and visible light (wIRA/VIS) treatment reduces *Chlamydia caviae*-induced ocular inflammation and infectious load in a Guinea pig model of inclusion conjunctivitis, J. Photochem. Photobiol. B 209 (2020) 111953.
[22] P.C. Ikwegbue, P. Masamba, B.E. Oyinloye, A.P. Kappo, Roles of heat shock proteins in apoptosis, oxidative stress, human inflammatory diseases, and cancer, Pharmaceuticals (Basel) (2017) 11.
[23] D.J. Miller, P.E. Fort, Heat shock proteins regulatory role in neurodevelopment, Front. Neurosci. 12 (2018) 821.
[24] D.M. Guttmann, C. Koumenis, The heat shock proteins as targets for radiosensitization and chemosensitization in cancer, Cancer Biol. Ther. 12 (2011) 1023–1031.
[25] A. Paul, S. Wilson, C.M. Belham, C.J. Robinson, P.H. Scott, G.W. Gould, R. Plevin, Stress-activated protein kinases: activation, regulation and function, Cell. Signal. 9 (1997) 403–410.
[26] S. Belij-Rammerstorfer, A. Inic-Kanada, M. Stojanovic, E. Marinkovic, I. Lukic, E. Stein, J. Montanaro, N. Bintner, N. Schürer, E. Ghasemian, et al., Infectious dose and repeated infections are key factors influencing immune response characteristics in guinea pig ocular chlamydial infection, Microbes Infect. 18 (2016) 254–262.
[27] A. Frohns, F. Frohns, S.C. Naumann, P.G. Layer, M. Löbrich, Inefficient double-strand break repair in murine rod photoreceptors with inverted heterochromatin organization, Curr. Biol. 24 (2014) 1080–1090.
[28] R.C. Team, R: A Language and Environment for Statistical Computing, R Foundation for Statistical Computing, 2016.
[29] R.G. Rank, J.A. Whittum-Hudson, Animal models for ocular infections, Methods Enzymol. 235 (1994) 69–83.
[30] R.G. Rank, In Vivo Chlamydial Infection. In Intracellular Pathogens I: Chlamydiales, American Society of Microbiology, 2012, https://doi.org/10.1128/9781555817329.ch13.
[31] A. Inic-Kanada, M. Stojanovic, S. Schlacher, E. Stein, S. Belij-Rammerstorfer, E. Marinkovic, I. Lukic, J. Montanaro, N. Schuerer, N. Bintner, et al., Delivery of a chlamydial adhesin N-PmpC subunit vaccine to the ocular mucosa using particulate carriers, PLoS One 10 (2015), e0144380.
[32] A. Filipovic, E. Ghasemian, A. Inic-Kanada, I. Lukic, E. Stein, E. Marinkovic, R. Djokic, D. Kosanovic, N. Schuerer, H. Chalabi, et al., The effect of infectious dose on humoral and cellular immune responses in *Chlamydophila caviae* primary ocular infection, PLoS One 12 (2017), e0180551.
[33] A. Inic-Kanada, E. Stein, M. Stojanovic, N. Schuerer, E. Ghasemian, A. Filipovic, E. Marinkovic, D. Kosanovic, T. Barisani-Asenbauer, Effects of iota-carrageenan on ocular *Chlamydia trachomatis* infection in vitro and in vivo, J. Appl. Phycol. 30 (2018) 2601–2610.
[34] H.M. Lacy, A.K. Bowlin, L. Hennings, A.M. Scurlock, U.M. Nagarajan, R.G. Rank, Essential role for neutrophils in pathogenesis and adaptive immunity in *Chlamydia caviae* ocular infections, Infect. Immun. 79 (2011) 1889–1897.
[35] I.V. Ivanov, T. Mappes, P. Schaupp, C. Lappe, S. Wahl, Ultraviolet radiation oxidative stress affects eye health, J. Biophotonics 11 (2018), e201700377.
[36] J. Voke, Radiation effects on the eye, part 1: infrared radiation effects on ocular tissue, Optom. Today 9 (1999) 22–28.
[37] M. Wakakura, W.S. Foulds, Response of cultured Müller cells to heat shock–an immunocytochemical study of heat shock and intermediate filament proteins in response to temperature elevation, Exp. Eye Res. 48 (1989) 337–350.
[38] E. Sekiyama, M. Saint-Geniez, K. Yoneda, T. Hisatomi, S. Nakao, T.E. Walshe, K. Maruyama, A. Hafezi-Moghadam, J.W. Miller, S. Kinoshita, et al., Heat treatment of retinal pigment epithelium induces production of elastic lamina components and antiangiogenic activity, FASEB J. 26 (2012) 567–575.
[39] T. Okuno, M. Kojima, S. Yamaguchi-Sekino, Y. Ishiba, Y. Suzuki, D.H. Sliney, Cataract formation by near-infrared radiation in rabbits, Photochem. Photobiol. 97 (2021) 372–376.
[40] A.M. Shah, A. Galor, Impact of ocular surface temperature on tear characteristics: current insights, Clin. Optom. (Auckl.) 13 (2021) 51–62.
[41] M.B. Landers 3rd, J.S. Watson, J.N. Ulrich, H. Quiroz-Mercado, Determination of retinal and vitreous temperature in vitrectomy, Retina 32 (2012) 172–176.
[42] F. Lorget, A. Parenteau, M. Carrier, D. Lambert, A. Gueorguieva, C. Schuetz, V. Bantseev, E. Thackaberry, Characterization of the pH and temperature in the rabbit, pig, and monkey eye: key parameters for the development of long-acting delivery ocular strategies, Mol. Pharm. 13 (2016) 2891–2896.
[43] J.L. Roti Roti, Cellular responses to hyperthermia (40-46 degrees C): cell killing and molecular events, Int. J. Hyperth. 24 (2008) 3–15.
[44] T. Mantso, S. Vasileiadis, I. Anestopoulos, G.P. Voulgaridou, E. Lampri, S. Botaitis, E.N. Kontomanolis, C. Simopoulos, G. Goussetis, R. Franco, et al., Hyperthermia induces therapeutic effectiveness and potentiates adjuvant therapy with non-targeted and targeted drugs in an in vitro model of human malignant melanoma, Sci. Rep. 8 (2018) 10724.
[45] E. Fehrenbach, H. Northoff, Free radicals, exercise, apoptosis, and heat shock proteins, Exerc. Immunol. Rev. 7 (2001) 66–89.
[46] L. Urbak, H. Vorum, Heat shock proteins in the human eye, Int. J. Proteomics 2010 (2010) 479571.
[47] M. Amirkavei, M. Pitkänen, O. Kaikkonen, K. Kaarniranta, H. André, A. Koskelainen, Induction of heat shock protein 70 in mouse RPE as an in vivo model of transpupillary thermal stimulation, Int. J. Mol. Sci. 21 (2020).
[48] M.J. Tsai, Y.L. Hsu, K.Y. Wu, R.C. Yang, Y.J. Chen, H.S. Yu, P.L. Kuo, Heat effect induces production of inflammatory cytokines through heat shock protein 90 pathway in cornea cells, Curr. Eye Res. 38 (2013) 464–471.
[49] C. Peterson, E. Driskell, D. Wilkie, C. Premanandan, R. Hamor, Heat-shock protein 70 expression in the equine cornea, Vet. Ophthalmol. 20 (2017) 344–348.
[50] L.M. Parver, C. Auker, D.O. Carpenter, Choroidal blood flow as a heat dissipating mechanism in the macula, Am J. Ophthalmol. 89 (1980) 641–646.
[51] Q. Zhu, S. Xiao, Z. Hua, D. Yang, M. Hu, Y.T. Zhu, H. Zhong, Near infrared (NIR) light therapy of eye diseases: a review, Int. J. Med. Sci. 18 (2021) 109–119.

[52] M. Migliario, M. Sabbatini, C. Mortellaro, F. Renò, Near infrared low-level laser therapy and cell proliferation: the emerging role of redox sensitive signal transduction pathways, J. Biophotonics 11 (2018), e201800025.
[53] B. Yao, S. Wang, P. Xiao, Q. Wang, Y. Hea, Y. Zhang, MAPK signaling pathways in eye wounds: multifunction and cooperation, Exp. Cell Res. 359 (2017) 10–16.
[54] W. Lan, A. Petznick, S. Heryati, M. Rifada, L. Tong, Nuclear factor-κB: central regulator in ocular surface inflammation and diseases, Ocul. Surf. 10 (2012) 137–148.
[55] J. Stone, D. van Driel, K. Valter, S. Rees, J. Provis, The locations of mitochondria in mammalian photoreceptors: relation to retinal vasculature, Brain Res. 1189 (2008) 58–69.
[56] J. Vicente-Tejedor, M. Marchena, L. Ramírez, D. García-Ayuso, V. Gómez-Vicente, C. Sánchez-Ramos, P. de la Villa, F. Germain, Removal of the blue component of light significantly decreases retinal damage after high intensity exposure, PLoS One 13 (2018), e0194218.
[57] C. Sivapathasuntharam, S. Sivaprasad, C. Hogg, G. Jeffery, Aging retinal function is improved by near infrared light (670 nm) that is associated with corrected mitochondrial decline, Neurobiol. Aging 52 (2017) 66–70.
[58] P.V. Algvere, J. Marshall, S. Seregard, Age-related maculopathy and the impact of blue light hazard, Acta Ophthalmol. Scand. 84 (2006) 4–15.
[59] M. García, E. Vecino, Role of Müller glia in neuroprotection and regeneration in the retina, Histol. Histopathol. 18 (2003) 1205–1218.